Mechanical Testing and Diagnosis
ISSN 2247 – 9635, 2022 (XIi), Volume 1, pp. 12-19

THE INFLUENCE OF BONDING TYPE OF TWO TARGET MODELS

Larisa CHIPER TITIRE, George Ghiocel OJOC, Cristian MUNTENIȚĂ, Lorena DELEANU

[2]**"Dunarea de Jos" University of Galati, , Romania**

e-mail: george.ojoc@ugal.ro

ABSTRACT

This paper compares two models for ballistic impact on unidirectional fabrics in order to evaluate their influence in making the simulation closer to actual events.
The importance of including the effect of fibers and yarns architecture, their properties and those for their matrix in the model is highlighted by figures showing equivalent stress distributions at different moments of the impact and images from the run simulations. It resulted that the model with interlaminar delamination is more suitable for these simulations considering the stress distribution analyzed for the main yarns of the panel.

Keywords: *simulation, finite element method, ballistic impact, unidirectional fabrics, interlaminar delamination*

1. INTRODUCTION

The materials and technology involved in creating protective systems, as well as the quantity of tests necessary to evaluate system performances, testing campaigns in ballistics are particularly expensive and time-consuming. This is why engineers can restrict the parameter ranges by simulating the behavior of the relevant system [1]. To create a model that behaves as closely as possible to reality is the main challenge.

The main challenge is to create a model that behaves as closely as possible to reality. The steps involved in creating a protective system typically include documentation, system design, mechanical tests that could aid in comparing the characteristics with those of existing systems.

Aramid fibers have ballistic applications especially for lightweight fabrics and composites, used in particular applications as flexible body armor, breastplates, helmets, protections for helicopters, military cargo planes, high-speed coast guard boats [2]. This is why researchers are interested in these types of fabrics and they alternate simulations with actual tests in order to accelerate the design of new products.

Based on actual and computer-simulated data, the design might be enhanced while taking into account many factors including surface density, worker comfort, production time, price, etc.

2. MODELING

This paper presents the results of the impact between a projectile made of two bodies (the jcket, which is made of copper alloy and the core, made of lead alloy) and a target made of 8 layers with wires oriented unidirectionally (layers with wires oriented at 0 and layers with fire oriented at 90). The two bodies that form the projectile have a connection between them that is "perfectly bonded".

Since the model is made up of yarns that are considered to form a single homogeneous, isotropic material, this scale model is meso. The projectile and the wires forming the target have the same geometry for the two cases studied in this paper, with the yarns having a thickness of 0.2 mm, a width of 3 mm, and a length of 180 mm.

The two cases studied in this paper are:

- case 1 which considers between yarns only friction, as well as friction between projectile and yarns,
- case 2 which has a zone of cohesion of zero thickness between the two layers, formed by unidirectional yarns, but also friction, the condition between the yarns being "bonded".

The two cases studied for moving bodies in the frictional contact condition. The coefficient of friction is considered constant and has a value of 0.3.

Figure 1 shows the model of the projectile, which has the same dimensions as the model used by [3]. The running time is 1×10^{-4} s. The model is run on the sphere, which lead to the presence of two assumed symmetry planes are preserved during the simulations.

The cross section of the yarns was modeled as a rectangular section. The yarns are clamped at the ends for a length of 3 mm in the direction of the length of the yarn (Fig. 3).

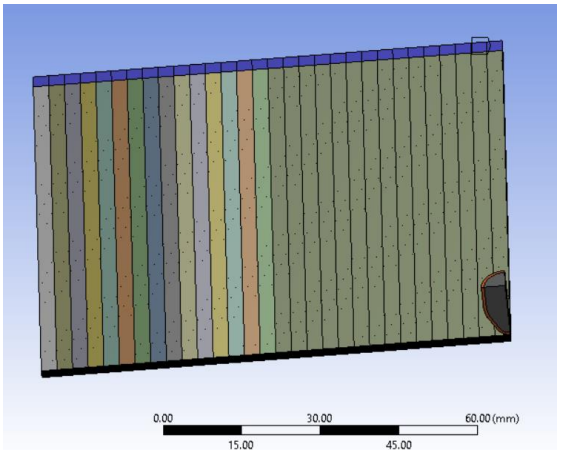

Fig. 1. The geometry of the model.

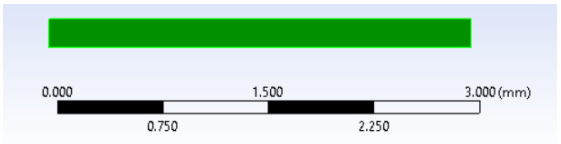

Fig. 2. The cross section of the yarns.

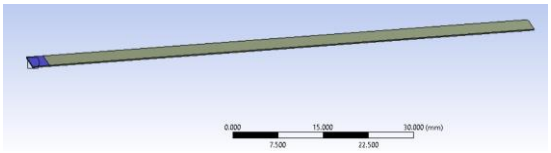

Fig. 3. Clamping of the yarn.

The projectile's properties are listed in Table 1 and the yarn's properties are shown in Table 2. Since the model is isothermal, the temperature is fixed at 22°C for all characteristics.

Table 1. Mechanical properties for materials the projectile jacket and core are made of

Property	Jacket (Copper alloy NL)	Core (Lead alloy)
Density [kg mm^-3]	8.3e-6	.134e-5
Specific heat at constant pressure [mJ/(kg °C]	3.85e+5	l.24e+5
Young modulus [MPa]	1.1e+5	16000
Poisson coefficient	0.34	0.44
Bilinear Isotropic Hardening		
Yield Strength [MPa]	280	30
Tangent Modulus [MPa]	1150	110
Equivalent plastic strain at break	0.75	0.75

Table 2. Mechanical properties of a yarn

Property	Value
Density [kg/mm^3]	1.44e+3
Young modulus [MPa]	6.5e+4
Poisson coefficient	0.35
Temperature [°C]	22
Isotropic bilinear hardening model	
Initial yield limit [MPa]	630
Tangent modulus [MPa]	1900
Equivalent plastic strain at break	0.1

In Tables 3 and 4 are given the values that were used for the tensile stress and the shear stress that characterize the resin matrix, because these values tell us if the bond imposed between the wires is broken, taking into account [4]-[8].

The "Path" function of Explicit Dynamics (Fig. 5) is used to determine the differences between the two situations examined are described based on the stress distributions on the primary yarns (the yarns in contact with the projectile during impact) on each layer (Fig. 4).

Table 3. Parameters for modeling the bilinear strength in interlaminar delamination

Maximum normal stress at traction, MPa	Normal displacement jump at completion of debonding, mm	Maximum tangential stress at traction, MPa	Tangential displacement jump at completion of debonding, mm	Ratio
70	5	50	0.1	0.3

Table 4. Parameters for energy at break in delamination

Maximum normal contact stress, MPa	Critical fracture energy for normal separation, J/m^2	Maximum equivalent tangential contact stress, MPa	Critical fracture energy for tangential slip, J/m^2	Artificial damping coefficient, s
100	3000	-	-	0.1

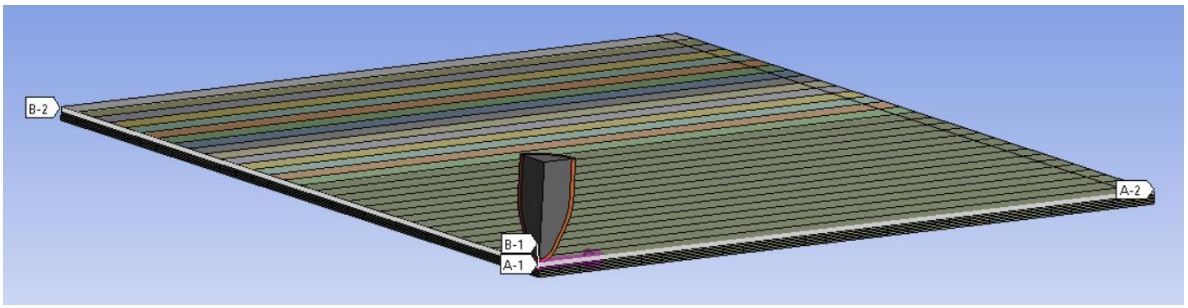

Fig. 5. The "Path" function of Explicit Dynamics

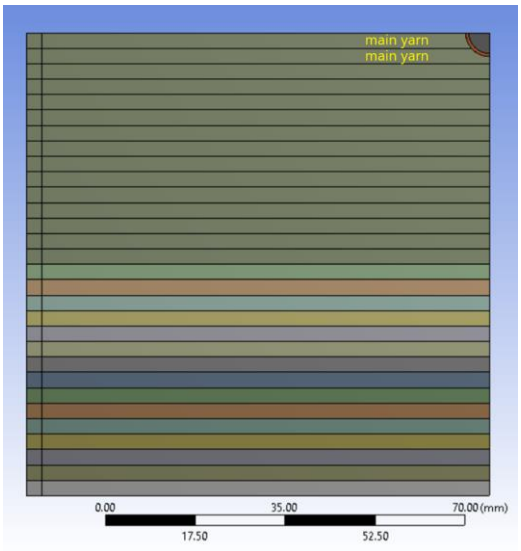

Fig. 4. Notation for the yarn

3. RESULTS

The results are presented both for the case with friction between the yarns and friction between the projectile and the yarns, as well as for the case with a cohesion zone between two yarns and friction in order to be able to discuss aspects by highlighting the differences in the stress distribution on the main yarns of each layer in impact time at different time points.

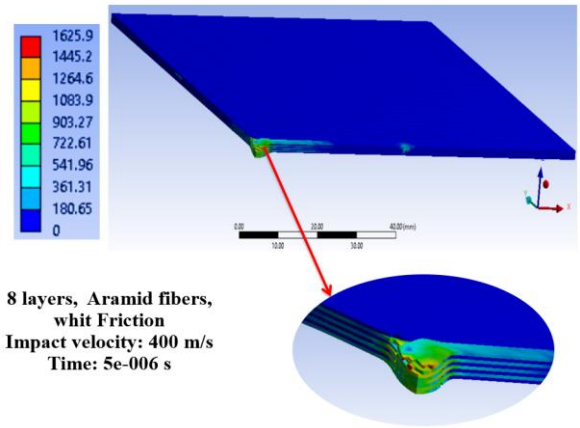

Fig. 6. von Mises stress distributions (in MPa), for case with interlaminar delamination, at moment $t=5\times10^{-6}$ s

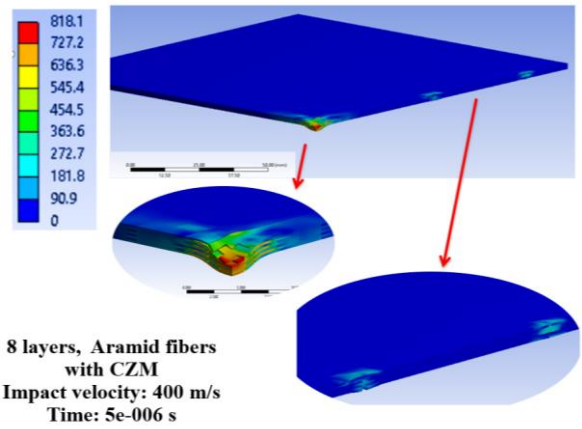

Fig. 7. von Mises stress distributions (in MPa), for the case with interlaminar delamination model and friction , at moment $t=5\times10^{-6}$ s

First moment of impact, $t=5\times10^{-6}$, shows that the model with CZM and friction has the main yarns 1 already broken in the first three layers, the break being caused by the bullet compression (Fig. 6). The model with friction only has broken yarns only in the first two layers, but the failure process is the same (compression) (Fig. 7). The von Mises stress distribution on these main yarns 1 is higher for the model that included only friction.

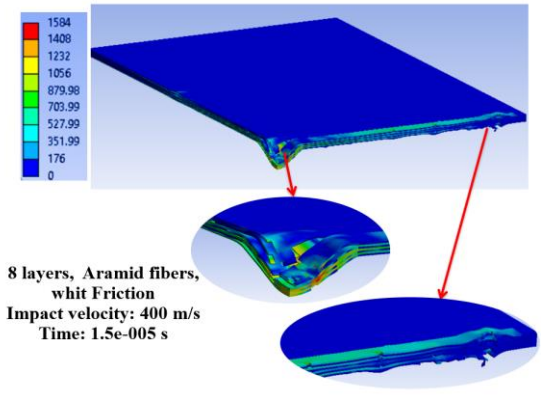

Fig. 8. von Mises stress distributions (in MPa) for the case with friction, at moment $t = 1.5 \times 10^{-5}$ s

At moment $t=1.5x10^{-5}$ s, the von Mises stress decreases at 1580 MPa for the model with friction only, the main yarns on 5 five successive layers are broken under the projectile. These main yarns are

tensioned till their fixed ends and begin to have distance between layers due to energy absorption.

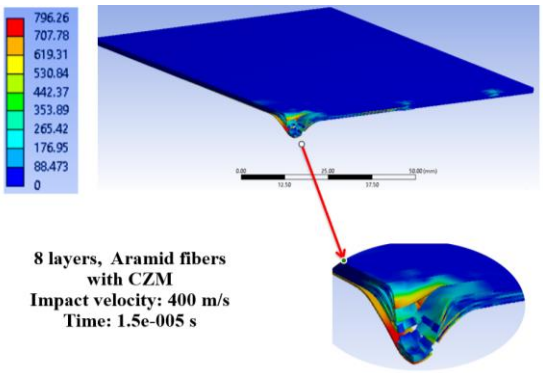

Fig. 9. von Mises stress distributions for case (in MPa) With cohesive zone model and friction, at moment t=1.5×10^{-5} s

At time t=1.5×10^{-5} s, for the model with CZM, the stress increases to 796 MPa, 7 layers are already broken, the last layer is highly stressed, the main yarns are tensioned up to approximately half of the length of the yarn. The yarns start to bend (main yarn 1) and lengthwise (main yarn 2) and begin to peel off.

The results in Figures 12 and 13 are presented for the friction aramid fiber fabrics and for the friction aramid fiber and CZM model, and particular aspects are discussed by highlighting the differences in the stress distribution on two main yarns of each layer at different points in time.

For the second moment of the simulation, t=1×10^{-5} s, the stress distribution along the half-length of the main yarn 1, the breaking of the first 3 layers made of aramid fibers, in the case with only friction (Fig. 12). The curve for the equivalent stress drops to zero when the yarn is broken. For the model with aramid fiber yarns, the main yarns 1 are broken in the first 4 layers and lower von Mises stress values are observed for the model with friction aramid fiber yarns and CZM.

The lack of layers' bond by a cohesive zone model introduces many aspect differences in the graphs of von Misses stress along main yarns, as presented in Fig. 12.

For the first moment, t=1×10^{-5} s, the existence of bonding conditions and the failure conditions as given in Tables 1 and 4, the von Mises stress distribution are concentrated around the impact in a zone of a length of about 20 mm along from the yarn length and from the geometrical axis of the model (panel and projectile). As von Mises stress is zero for main yarns 1 on layers 1 and 3, it means these are already broken (failed). Also, higher values appear along the yarns. For the panel model with only friction, the same yarns are broken but it is visible that

For the case with only friction, the number of broken yarns (main yarns 1) are the same but the yarns on the following layer have higher values for the equivalent stress supposing a more intense failure in the next moment as the values are close to the strength limit.

The main yarns 2 (with 0° orientation) are not failed yet on the model with CZM, but for the case with only friction, the main yarn 2 on layer 1 has been already broken and the main yarn 2 on layer 3 has a very high value for von Mises stress, suggesting a future break

The graphs for the main yarn 1 on the layers with even number suggest that main yarn 1 on layer 2 is broken, and it is visible the fragmentation of this yarn as there are three points of zero stress (the model is represented by a quarter of the panel and the projectile. But that on layer 4 has values near the strength limit of the yarn.

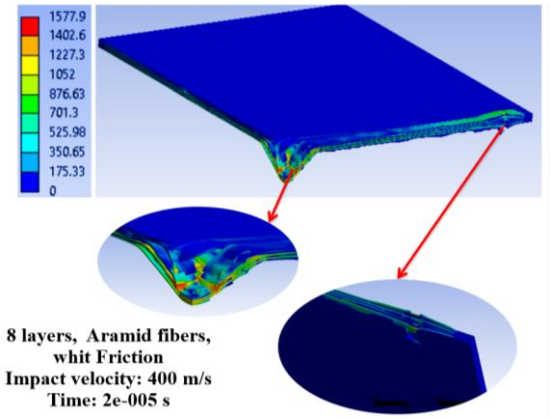

Fig. 10. von Mises stress distributions (in MPa), for the case with friction only, at moment $t = 2 \times 10^{-5}$ s

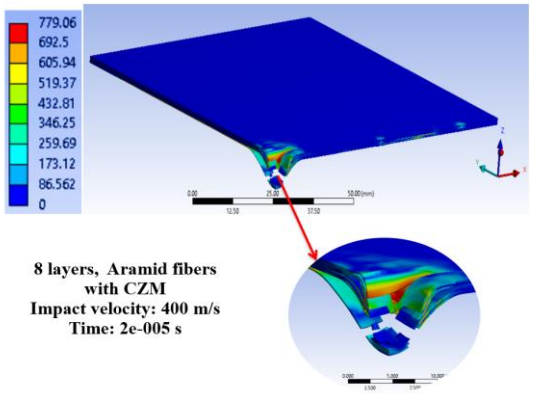

Fig. 11. von Mises stress distributions for case (in MPa) with cohesive zone model and friction, at moment t=2×10^{-5} s

For the model with only friction among yarns, the yarns that wave been impacted, induct the absorbed energy along, then, producing waves in the yarns shape (Fig. 11) that generate higher bending moments towards the fixed ends of yarns. These bending moments could produce the break of the yarns near their fixed ends. When introducing CZM, the waving process of yarns is very much attenuated and even the stress distribution is not so high near the yarns ends (weaving bending is very much reduced). Another

visible effect of CZM is that it can print out the delamination process that could be tuned by the mechanical characteristic that are attached to the model by user, based on experimental data in actual stratified system.

Comparing Fig. 10 to Fig. 11, one may notice that the absence of bonding generates high bending stress and the separation of layers on the entire panel. When the layers are bonded in the condition described in the model with CZM, high stresses are localized in the impact region and the dynamics of yarns' failure are more rapidly, as revealed by the simulation.

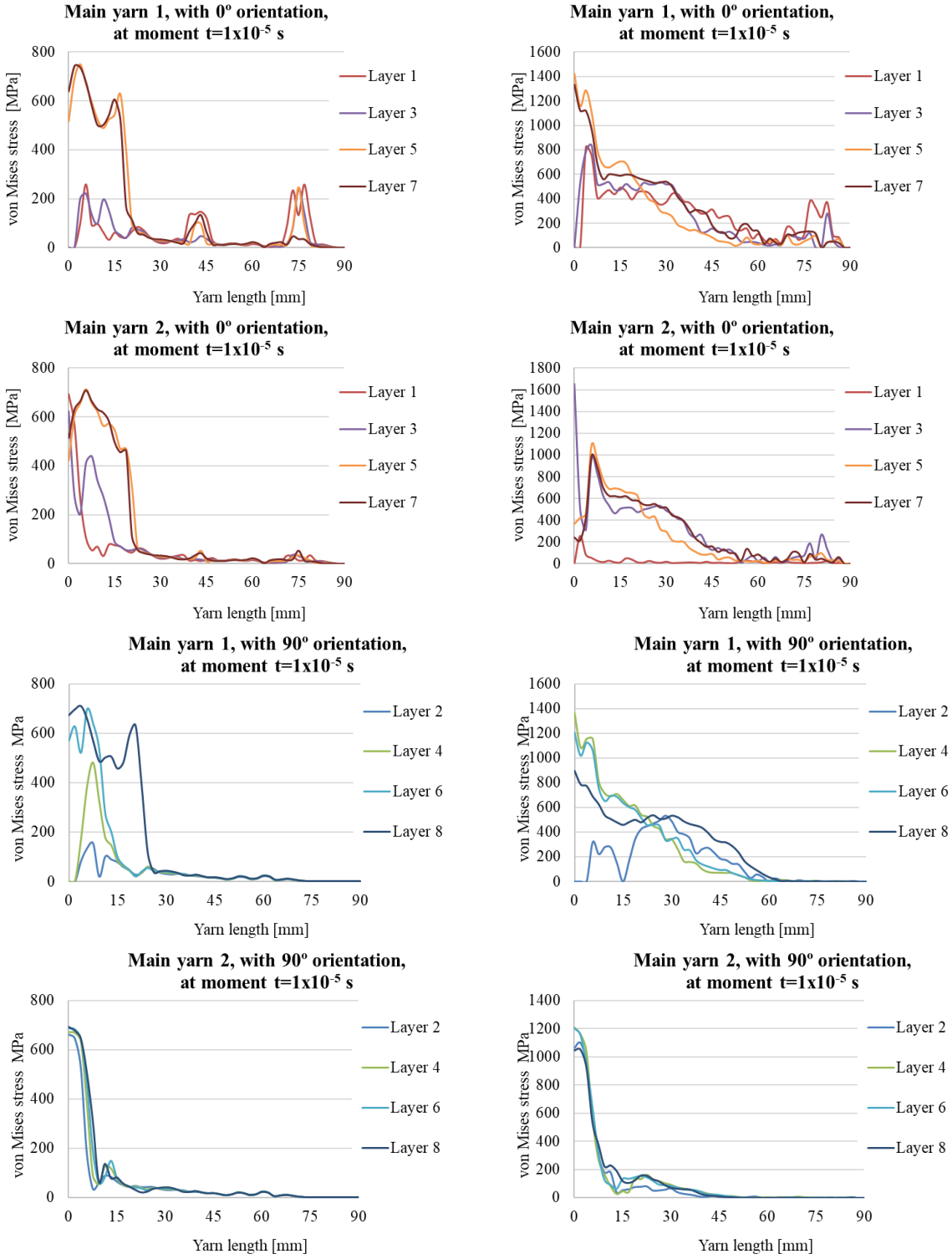

a) with friction and interlaminar delamination b) with friction only

Fig. 12. von Mises stress distributions, at moment t=1×10^{-5} s

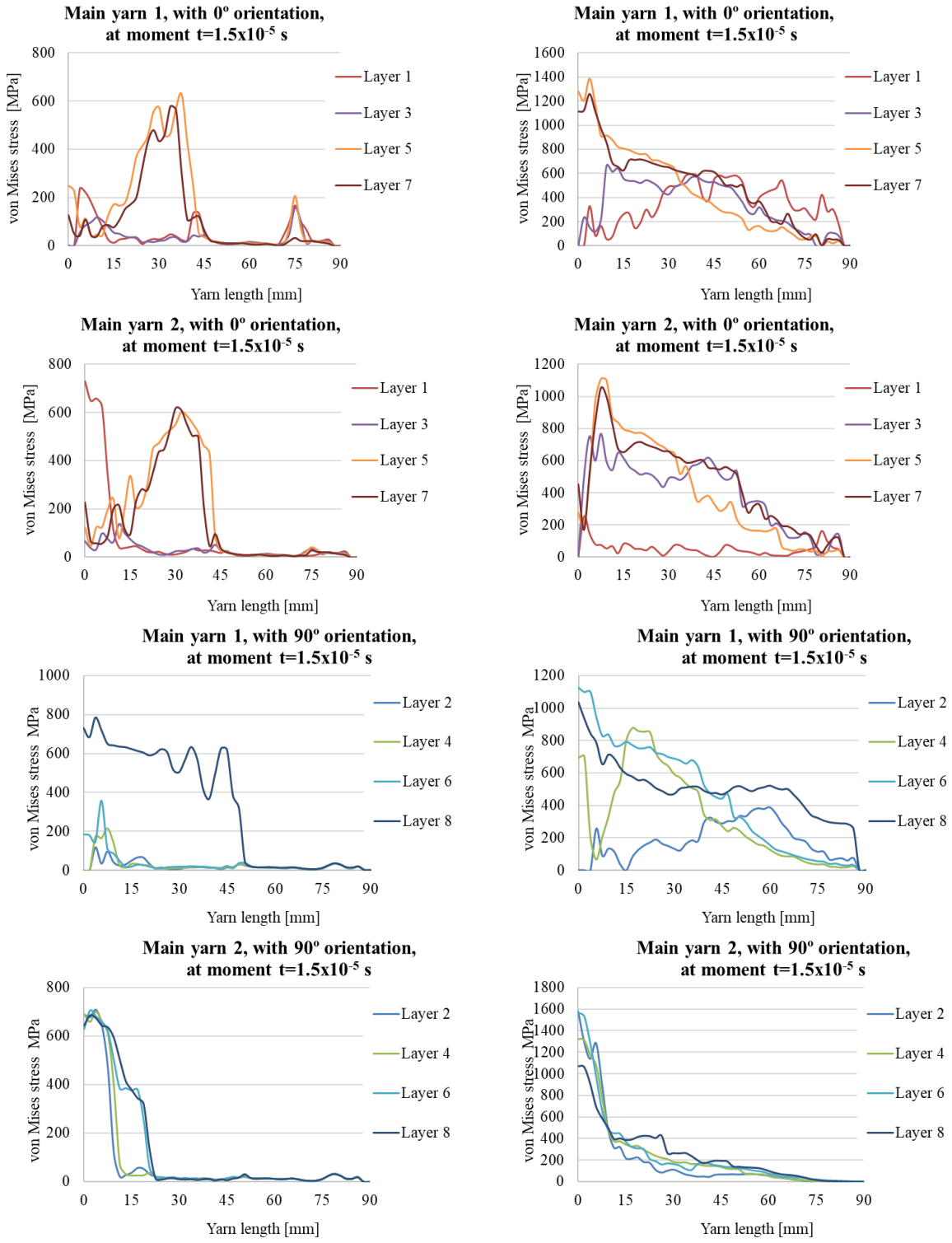

a) with friction and cohesive zone model b) with friction

Fig. 13. von Mises stress distributions, at moment t=1.5×10^{-5} s

The results are presented for the time instant t=1.5×10^{-5} s, in Fig. 13. In only 0.5×10^{-5} s, the aspect of von Mises stress is different, pointing out the dynamics of the impact. The main yarns 1 oriented at 0° are broken on layer 1 and start on layer 3 and the main yarns 2 are not yet broken for the aramid fiber model with friction. For the model with aramid fiber with friction and with CZM, the main yarns 1 oriented at 0° are broken on layers 1 and 3 and the main yarns 2 are not broken. The main yarns 1 oriented at 90° for the model with friction and CZM are broken on layers 2 and 4 and for the model with friction, the main yarn 1 oriented at 90° is broken only on layer 2. For both cases, the main yarns 2 are not broken.

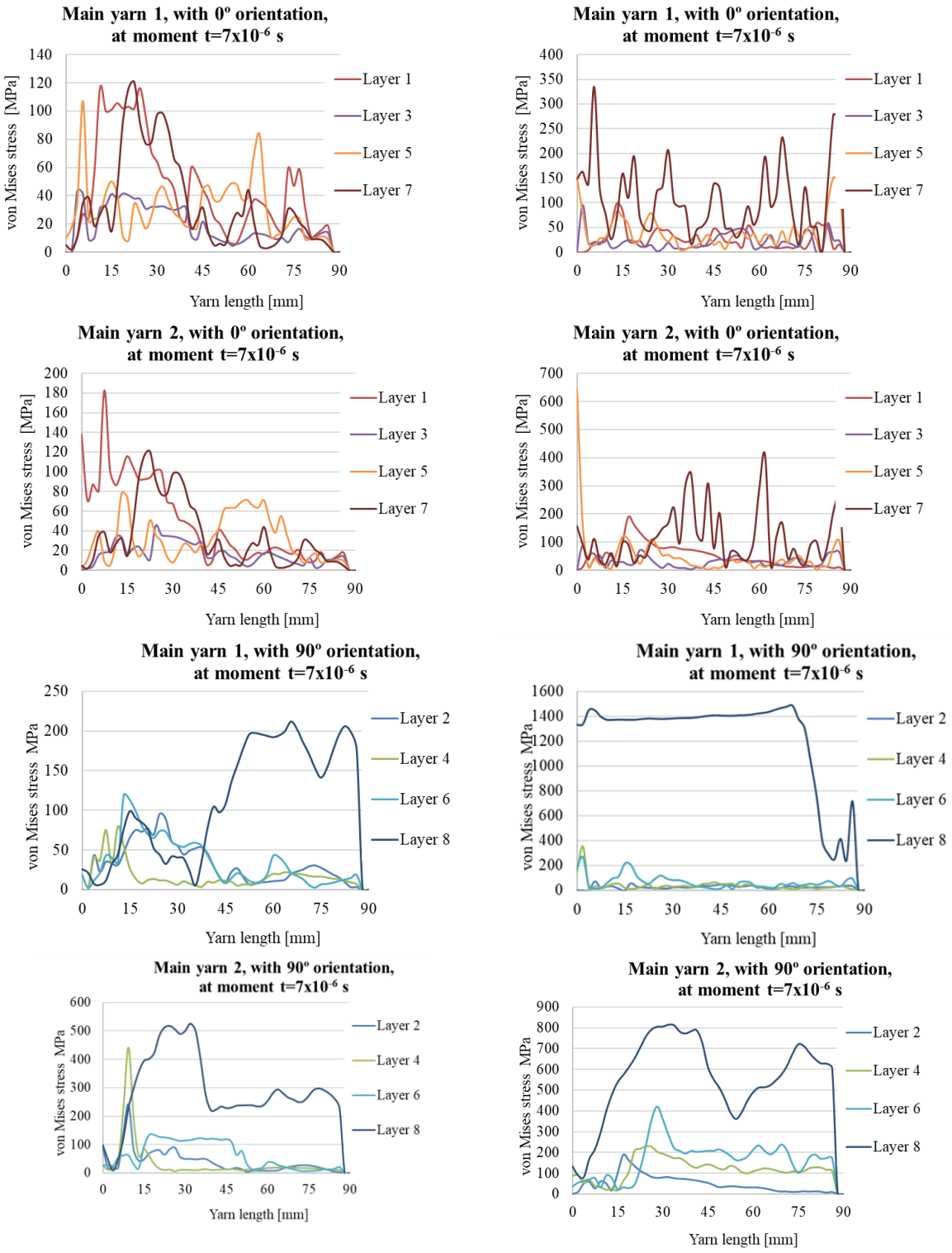

a) with friction and cohesive zone model b) with friction

Fig. 13. von Mises stress distributions, at moment t=1.5×10^{-5} s

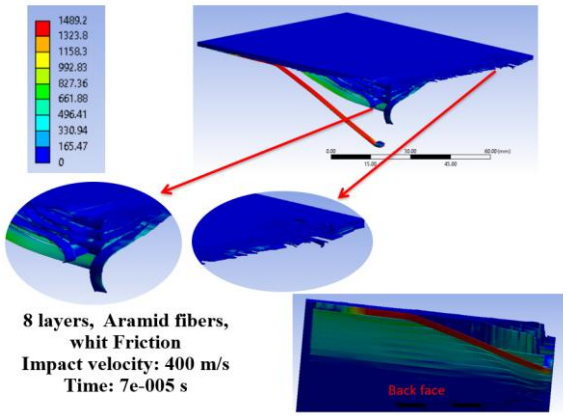

Fig. 14. von Mises stress distributions for case (in MPa) friction, at moment $t=7\times10^{-5}$ s

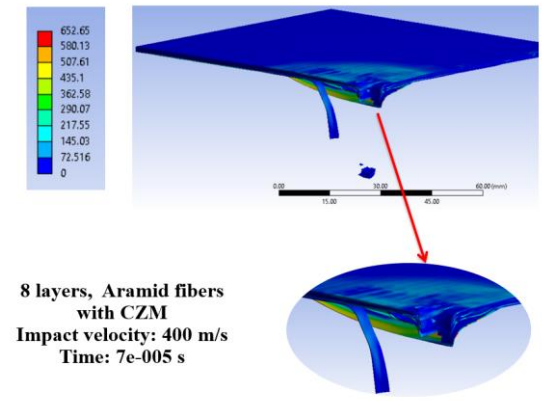

Fig. 15. von Mises stress distributions for case (in MPa) With cohesive zone model and friction, at moment $t=7\times10^{-5}$ s

4. CONCLUSIONS

The importance of including the effect of fibers and yarns architecture, their properties, and those for their matrix in the model is highlighted by figures showing equivalent stress distributions, at different moments of the impact and photos from the run simulations.

These models are useful in narrowing the test parameters for assessing the safety of materials and designed systems against a certain threat.

REFERENCES:

1. *** Opportunities in Protection Materials Science and Technology for Future Army Applications (2011), http://nap.edu/13157
2. Bhatnagar A. (editor) (2016) *Lightweight Ballistic Composites Military and Law-Enforcement Application*s, Second Edition
3. Wiśniewski, A., Gmitrzuk, M. (2014) Validation of numerical model of the Twaron CT709 ballistic fabric, *Problems of Mechatronics, Armament, Aviation, Safety Engineering*, **5,** 2(16), pp. 19-32
4. Joki, R. K., Grytten, F., Hayman, B., & Sørensen, B. F. (2016). Determination of a cohesive law for delamination modelling - Accounting for variation in crack opening and stress state across the test specimen width. *Composites Science and Technology*, **128,** 49-57. 10.1016/j.compscitech.2016.01.026
5. Chowdhury, U., & Wu, X.-F. (2021) Cohesive zone modeling of the elastoplastic and failure behavior of polymer nanoclay composites. *Journal of Composites Science*, **5**, 131. https://doi.org/10.3390/jcs5050131
6. *** ANSYS Explicit Dynamics Analysis Guide (2021). ANSYS, Inc., USA
7. Năstăsescu V., Ştefan A., Lupoiu C., *Analiza neliniară prin metoda elementelor finite. Fundamente teoretice şi aplicaţii* (in Romanian), Academia Tehnică Militară, Bucureşti, 2001.
8. Jinescu, V. V. (2015) *Application in Mechanical Engineering of Principle of Critical Energy*, Lambert Academic Publishing, Saarbrücken, Germany